New Physics: Sae Mulli,
Vol. 68, No. 5, May 2018, pp. 563∼569
http://dx.doi.org/10.3938/NPSM.68.563

Check for updates

Role of Cutoff Scaling in Scale-Free Networks

Meesoon HA*
Department of Physics Education, Chosun University, Gwangju 61452, Korea

(Received 31 March 2018 : revised 20 April 2018 : accepted 24 April 2018)

We numerically study how the cutoff scaling of the upper degree affects the finite-size scaling (FSS) for physical models of scale-free networks (SFNs) in terms of the Ising model for annealed and quenched SFNs. Based on the hyperscaling argument and the results of S. H. Lee *et al.* [Phys. Rev. E **80**, 051127 (2009)], we test the suggested FSS theory according to the value of the cutoff exponent, and find the cutoff of upper degree scales as a power law in the system size. In particular, we focus on finding the relevant length scale in finite SFNs near and at criticality. Moreover, we investigate the self-averaging property of the system in the presence of a quenched linking disorder as a way for exploring the fluctuations in the sampling disorder for the finite-degree sequence set.

PACS numbers: 05.70.Jk, 64.60.-i, 89.75.Fb, 89.75.Hc
Keywords: Critical phenomena, Cutoff scaling, Annealed and quenched scale-free networks, Finite-size scaling, Self-averaging property

I. INTRODUCTION

To study critical phenomena and phase transitions in random scale-free networks (SFNs) [1–5] are not only interesting but also important in many aspects of real systems since the degree heterogeneity is one of essential ingredients determining the universality class [6].

However, there still remains a subtle issue for the finite-size scaling (FSS) theory in SFNs. In a SFN with finite N nodes and the power-law degree distribution $P(k) \sim k^{-\lambda}$, the upper cutoff of degrees (the maximum degree) scales as $k_c \sim N^{1/\omega}$. For instance, the configuration model [7] has a "natural" cutoff $k_c \sim N^{1/\omega_{\rm nat}}$ with $\omega_{\rm nat} = \lambda - 1$. In general, a SFN model can have an arbitrary cutoff exponent $\omega \geq \omega_{\rm nat}$. The power-law scaling $k_c \sim N^{1/\omega}$ indicates that SF networks with the same λ but with different ω may follow different routes to the thermodynamic limit $N \to \infty$. Hence, one may suspect that the exponent $\bar{\nu}$ describing the finite size effect depends not only on λ but also on ω.

The analytic and numerical results for simple physical models in Ref. [8] seem to exclude such a possibility that $\bar{\nu}$ may depend on ω in *quenched* SFNs [1].

It has been reported that the simplest one among nonequilibrium models, contac process (CP), on *annealed* SFNs does exhibit ω-dependent FSS behaviors [9, 10]. In an *annealed* network, edges are fluctuating and interact with all the other nodes probabilistically. The annealed approach is very useful since the mean-field (MF) theory becomes exact and analytically tractable even for finite N. As a result, it is found that the CP on annealed SFNs with $2 < \lambda < 3$ and $\omega > \omega_{\rm nat}$ has two characteristic size scales $\xi_* \sim \epsilon^{-\bar{\nu}_*}$ and $\xi_c \sim \epsilon^{-\bar{\nu}_c}$ with $\bar{\nu}_* = \omega/(\lambda-2)$ and $\bar{\nu}_c = 2\omega/[\omega-(3-\lambda)]$, respectively [9,10], where $\bar{\nu}_* > \bar{\nu}_c$ and $\xi_* \gg \xi_c$. The system does not suffer from any finite size effect when $N \gg \xi_*$. In the range of $\xi_c < N < \xi_*$, the system behaves as if it were an infinite system but with a finite degree cutoff k_c. When $N \ll \xi_c$, it eventually behaves like a finite system with k_c, which clearly shows that the thermodynamic limiting behavior of the CP on annealed SFNs depends on k_c as $N \to \infty$.

The peculiar behavior of the CP on *annealed* SFNs raises some theoretical issues for the *quenched* case. It is

[1] A quenched network refers here to a network whose nodes and edges are fixed while dynamic variables (particles or spins) are fluctuating.

*E-mail: msha@chosun.ac.kr

not yet fully understood why they display the different FSS property. For the quenched case, edges themselves act as quenched random disorder, so it may play a crucial role in the FSS of the CP. Regarding such a discrepancy of the critical behavior between two cases, we pose another interesting question: Is the ω-dependent FSS property a generic feature of annealed SFNs or a specific feature of a nonequilibrium system? To answer the question, the annealed network version of the Ising model has been investigated in Ref. [11], where the FSS property for the annealed case for the simplest one of equilibrium models is compared with the quenched case by analytical and numerical methods.

In this paper, we revisit the annealed version of the Ising model in the context of the numerical data analysis, and discuss the fluctuations of sampling as the cutoff scaling setups vary.

This paper is organized as follows. We describe how to define the annealed version of the Ising model and show how to generate an annealed network in Sec. II, where the network basic properties are discussed as well as the self-averaging tests from sample flutuations. In Sec, III, the FSS theory is summaruzed with the conjecture according to the degree exponent of SFNs, which is numerically confirmed. We conclude this paper with summary and some remarks in Sec. IV.

II. MODEL

We consider the globally connected (GC) version of the Ising model on "annealed" SFNs. It is described by the following Hamiltonian,

$$\mathcal{H} = -\frac{1}{2}\sum_{i\neq j}\frac{k_i k_j}{N\langle k\rangle}s_i s_j. \qquad (1)$$

It is noted that all the spins interact with all the others in the GC version, but each interaction strength (coupling constant) is proportional to the products of degrees of the nodes at which the chosen spins are located.

In the thermodynamic limit ($N \to \infty$), Eq. (1) is exactly solvable by using the MF theory with the order parameter $m = \sum_k kP(k)m(k)/\langle k\rangle$, where $m(k) = \langle s_i\rangle$ for the set of node $\{i \mid k_i = k\}$. As a result, we obtain the following self-consistent equation:

$$m = \sum_k \frac{kP(k)}{\langle k\rangle}\tanh(mk/T). \qquad (2)$$

We can also consider the Landau free energy of m near the critical point T_c in the MF regime as

$$f(m) = -\epsilon m^2 + bm^4 + O(m^6), \qquad (3)$$

where the Gaussian spatial fluctuation term $(\nabla m)^2$ is ignored, $\epsilon \equiv (T_c - T)/T_c$ (the reduced temperature) and $b \equiv \langle k^4\rangle/\langle k^2\rangle^2$ (the quantity of our primary interest in this study).

Unless the fourth moment of $P(k)$ diverges, $\langle k^4\rangle \to \infty$ as $N \to \infty$, the series expansion of $\tanh(x) = x - x^3/3 + ...$ near $m = 0$ immediately shows that the critical behavior is the same as the standard MF theory of the original Ising model. As a result, we get the values for the critical exponents: $\beta = 1/2, \bar{\nu} = 2$, and $\gamma = 1$ (independent of λ) for $\lambda > 5$, which are from $m \sim \epsilon^{\beta}$, $\xi_v \sim \epsilon^{-\bar{\nu}}$, and $\chi_2 \sim \epsilon^{-\gamma}$ at the critical temperature $T_c = \langle k^2\rangle/\langle k\rangle$. For $3 \le \lambda \le 5$, the critical exponents becomes λ-dependent (it may also depend on the cutoff scaling exponent ω), but the critical temperature remains the same definition as $T_c = \langle k^2\rangle/\langle k\rangle$. Thus the result of T_c is very useful in the annealed network study.

For convenience sake, we denote, in the thermodynamic limit ($N = \infty$), $\langle A\rangle = \sum_{k_{\min}}^{\infty} AP(k)$, while for the finite network size N with $P_N(k)$, $\langle A\rangle_N = \sum_{k_{\min}}^{k_{\max}} AP_N(k)$.

1. Annealed SFNs

The SFN with a finite network size of N is described in terms of the degree distribution $P_N(k) = ck^{-\lambda}$ for $k_{\min} \le k \le k_{\max}$ with a normalization c and $P_N(k) = 0$ elsewhere. The minimum degree $k_{\min}$ is an $O(1)$ constant, while the maximum degree $k_{\max} = k_c$ scales with N as $k_c = aN^{1/\omega}$, with an $O(1)$ constant a. Since the neighbors of each node need not to be specified in the annealed version by definition, an annealed SFN is realized by choosing only a degree sequence $\{k_i\}$ for $1 \le i \le N$.

The degree sequence can be determined using the following two different ways: One is to assign degree k to N_k nodes **deterministically** as follows:

$$\sum_{k'>k} N_{k'} = \text{int}[N\sum_{k'\ge k} P(k')], \qquad (4)$$

for all k in the decreasing order from $k_{\max}$. Here $\text{int}[x]$ is the integer part of x. The other is to assign N_k against

k **stochastically** (probabilistically) in accordance with $P(k)$, which yield an ensemble of different networks. Therefore, the ensemble average is necessary and one should check sample fluctuations due to the sampling disorder. The relevant quantity to be discussed about the self-averaging property [12] is the coefficient b in the m^4 term in Eq. (3) with relative fluctuations R_b.

Consider both two methods in order to confirm "CP-like conjecture" for Ising model in annealed SFNs, which mimics that for the annealed version of CP [10], and corresponds to the simplest test for Ref. [11]. Before moving onto the main discussion, we briefly check network basic properties and the self-averaging issues.

2. Network Basic Properties

Annealed SFNs can be generated by three different ways, deterministically, stochastically, and Herrero-type deterministically, where we measure $P_{_N}(k)$, $\langle k^n\rangle_{_N}$, $T_c(N)$, and $b(N)$ for $\lambda = 4.0$ (all three cases) and $\lambda = 4.5$ (deterministic) with $a = 1$ and $a = 10$, except for the Herrero-type deterministic one where a is automatically determined [13].

For a given network, we use the temporal average in general for the better statistics of numerical data. In particular to the stochastic one, it is necessary to use the network realization average, so that the two types of ensemble averaging methods can be considered, namely *all* versus *survival* in analyzing data.

Mostly, our numerical results are comparable with analytical results. However, some discrepancy is noticeable due to strong finite size effects. In particular, for $3 < \lambda < 5$, at large $\omega > \lambda - 1$ (natural cutoff) with $a = 1$, $k_{\max} = N^{1/\omega}$ grow very slowly that it is quite difficult to observe the expected asymptotic scaling behavior since the values of $k_c(N)$ are too small to be distinguished for various N. To avoid this problem, we also consider the $a = 10$ case, but it turns out that there is another finite-size effect due to the small probability to generate $k_{\max}$ practically for large N.

3. Self-Averaging Tests

Unlike quenched SFNs where two kinds of disorder to be considered (one is from sampling a degree sequence, the sampling disorder, and the other is from choosing a way of linking nodes to create a network, the linking disorder), stochastic annealed SFNs only have the sampling disorder since it is free from the linking disorder by definition.

We test the self-averaging property in the stochastic annealed SFNs due to the sampling disorder. In this study, we focus on $b \equiv \langle k^4\rangle/\langle k^2\rangle^2$, where $\langle k^n\rangle = \sum_k k^n \tilde{P}(k)$ with a sampled degree distribution $\tilde{P}(k) = \sum_{i=1}^N \delta_{k,k_i}/N$.

Using the same technique as the self-averaging test of $g \equiv \langle k^2\rangle$ in the CP on annealed SFNs [10], we can calculate the quantity b of a given sample up to the second order as follows: $b = \frac{\langle k^4\rangle_0}{\langle k^2\rangle_0}\left(1 + \frac{\langle k^4\rangle_\delta}{\langle k^4\rangle_0} - 2\frac{\langle k^2\rangle_\delta}{\langle k^2\rangle_0} + 3\frac{\langle k^2\rangle_\delta^2}{\langle k^2\rangle_0^2} - 2\frac{\langle k^4\rangle_\delta \langle k^2\rangle_\delta}{\langle k^4\rangle_0 \langle k^2\rangle_0}\right)$, where $\langle k^n\rangle_0 \equiv \sum_k k^n P(k)$, and $\langle k^n\rangle_\delta \equiv \sum_k k^n \delta P(k)$, where $\delta P(k) = \tilde{P}(k) - P(k)$ (the deviation from the planned degree distribution $P(k)$ for $k_{\min} \le k \le k_{\max}$).

From the results of disorder-averaged correlators (see Eqs. (40)-(42) and (43) in Ref. [10]), we systematically expand $[b]$ and $(\Delta b)^2 = [b^2] - [b]^2$ in the powers of $\frac{1}{N}$, where $[\cdots]$ denotes the sampling disorder average. As a result, we obtain

$$[b] = \frac{\langle k^4\rangle_0}{\langle k^2\rangle_0^2}\left[1 + \frac{1}{N}\left(3\frac{\langle k^4\rangle_0}{\langle k^2\rangle_0} - 2\frac{\langle k^6\rangle_0}{\langle 2\rangle_0 \langle k^4\rangle_0} - 1\right)\right], \quad (5)$$

and

$$(\Delta b)^2 = \frac{1}{N}\frac{\langle k^4\rangle_0^2}{\langle k^2\rangle_0^4}\left(\frac{\langle k^8\rangle_0}{\langle k^4\rangle_0^2} - 4\frac{\langle k^6\rangle_0}{\langle k^2\rangle_0 \langle k^4\rangle_0} + 4\frac{\langle k^4\rangle_0}{\langle k^2\rangle_0^2} - 1\right). \quad (6)$$

The leading terms in Eqs. (5) and (6) are $[b] \sim \frac{\langle k^4\rangle_0}{\langle k^2\rangle_0^2}$, $(\Delta b)^2 \sim \frac{\langle k^8\rangle_0}{N\langle k^2\rangle_0^4}$, and $R_b \sim \frac{\langle k^8\rangle_0}{N\langle k^4\rangle_0^2}$, respectively. The scaling behaviors of $[b]$ and the relative fluctuations $R_b = (\Delta b)^2/[b]^2$ for $\lambda > 3$ and $\omega \ge \lambda - 1$ with $k_c = aN^{1/\omega}$ are expressed as

$$[b] = \begin{cases} \sim N^{(5-\lambda)/\omega} & \text{for } \ 3 < \lambda < 5 \\ \sim \log N & \text{for } \ \lambda = 5 \\ \sim O(1) & \text{for } \ \lambda > 5, \end{cases} \quad (7)$$

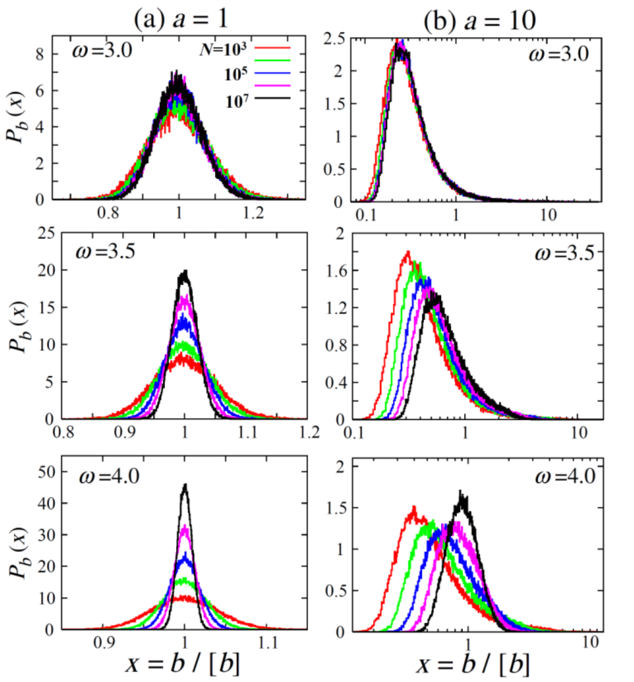

Fig. 1. (Color online) The normalized probability distribution $P_b(x)$ against $x = b/[b]$ in stochastic annealed SFNs with $N = 10^3, \cdots, 10^7$: (a) $a = 1$ and (b) $a = 10$ for $\lambda = 4.0$ with $\omega = 3.0$ (natural cutoff), 3.5, and 4.0 (Herrero-type strong cutoff [13]) from top to bottom. Numerical data are obtained from network realizations of 10^5 times.

and

$$R_b = \begin{cases} \sim N^{(\lambda-1)/\omega-1} & \text{for } \ 3<\lambda<5 \\ \sim N^{4/\omega-1}(\log N)^{-2} & \text{for } \ \lambda=5 \\ \sim N^{(9-\lambda)/\omega-1} & \text{for } \ 5<\lambda<9 \\ \sim N^{-1}\log N & \text{for } \ \lambda=9 \\ \sim N^{-1} & \text{for } \ \lambda>9. \end{cases} \tag{8}$$

The relative fluctuation R_b of b due to the sampling disorder (quenched type) plays a role of an indicator of the self-averaging property of the quantities related to b. For the self-averaging case, $R_b \sim N^{-\zeta}$, where $\zeta = 1$ is called as strongly self-averaging (SSA), and $0 < \zeta < 1$ is as weakly self-averaging (WSA). If the disorder is strong and relevant near the transition point, R_b approaches to a finite value as N increases, so that the system lacks the self-averaging property.

Eq. (8) tells us that for $\lambda \leq 9$ with $\omega > \lambda - 1$, R_b decays slower than SSA (N^{-1}), and the system in this range becomes WSA.

It is interesting that the system lacks the self-averaging property when $3 < \lambda < 5$ with $\omega = \lambda - 1$ ($R_b \to O(1)$ as N increases) since such a cutoff scaling behavior is observed in networks without any restrictions on the degree, namely the natural cutoff. Thus, the model study in the networks with the natural cutoff needs to consider not only the node-to-node degree fluctuations but also the strong sample-to-sample fluctuations.

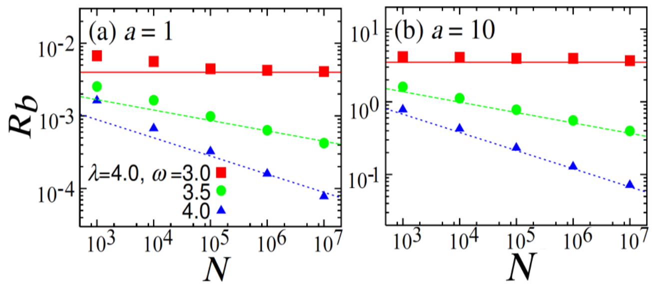

Fig. 2. (Color online) Double-logarithmic plots are shown for $R_b = ([b^2] - [b]^2)/[b]^2$ *vs.* N in stochastically gennerated annealed SFNs for $\lambda = 4.0$ for various cutoff exponents ω: (a) $a = 1$ and (b) $a = 10$. The straight lines represent theoretical predictions in Eq. (8), $R_b \sim N^{(\lambda-1)/\omega-1}$ for $3 < \lambda < 5$.

Fig. 1 shows the self-averaging property regarding b as constructing the probability density distribution $P_b(x)$ against $x = b/[b]$. In general, as ω increases, the width of P_b gets narrows. Moreover, we observe that it also does (but quite slow) as N increases for $\omega > \lambda - 1$ and it doesn't change (not self-averaging) at $\omega = \lambda - 1$, except for $N = 10^3$ (due to the finite-size effect). These facts can be confirmed when we plot R_b itself against N for various cases, see Fig. 2.

III. CONJECTURE AND NUMERICS

We perform extensive simulations in both deterministic and stochastic types of annealed SFNs for various values of the cutoff exponent ω and the coefficient a in $k_c = aN^{1/\omega}$ to test the critical and off-critical FSS, which tells us the three-regime scaling behavior for $3 < \lambda < 5$ if $\omega > \omega_{\text{nat}}$ and the two-regime scaling behavior otherwise.

First, we discuss the ω-dependent FSS theory of Ising model in annealed SFNs, which is originated from the scaling behavior of b for $3 < \lambda < 5/$, and call it "CP-like conjecture".

It is argued that at and near the critical point the order parameter of Ising model exhibits distinct scaling characteristics depending on whether $mk_{\max} > 1$ or $mk_{\max} < 1$

Table 1. Critical temperature and exponents ($y,\ 1/\bar{\nu}$) of Ising model on SFNs with $P(k) \sim k^{-\lambda}$ are summarized for the cutoff exponent ω, where $m \sim N^{-y}$ and $\epsilon \sim N^{-1/\bar{\nu}}$. For $\omega_{\text{nat}} = \lambda - 1$, $m \sim \epsilon^{\beta}$ with $\beta = \max[1/(\lambda-3), 1/2]$.

Network-type	T_c	λ	y	$1/\bar{\nu}$
Annealed	Exactly known as $\langle k^2\rangle/\langle k\rangle$	$3 < \lambda < 5$ if $\omega > \omega_{\text{nat}}$ otherwise	$m_x \sim N^{-y_x}$ $\frac{1}{4}\left(1+\frac{5-\lambda}{\omega}\right)$ (for m_c); $\frac{1}{\omega}$ (for m_*) $\frac{1}{\lambda-1}$ (since $m_c = m_* = m_q$)	$\epsilon_x \sim N^{-1/\bar{\nu}_x}$ $\frac{1}{2}\left(1-\frac{5-\lambda}{\omega}\right)$ (for ϵ_c); $\frac{\lambda-3}{\omega}$ (for ϵ_*) $\frac{\lambda-3}{\lambda-1}$ (since $\epsilon_c = \epsilon_* = \epsilon_q$)
Quenched	Numerically found	$3 < \lambda < 5$ (independent of ω)	$m_q \sim N^{-y_q = \beta/\bar{\nu}}$ $\frac{1}{\lambda-1}$	$\epsilon_q \sim N^{-1/\bar{\nu}}$ $\frac{\lambda-3}{\lambda-1}$
Both		$\lambda > 5$	$1/4$	$1/2$

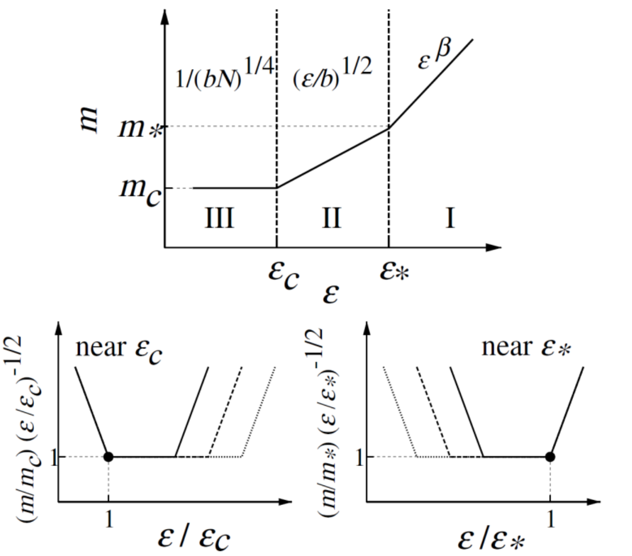

Fig. 3. Schematic plots of m *vs.* ϵ in annealed SFNs as double-logarithmic scales. The lower panel plots show how to collapse numerical data, where the different line type corresponds to the result of the different N value: (left) near ϵ_c, N gets larger from left to right, and (right) near ϵ_*, N gets larger from right to left, respectively.

in annealed SFNs as

$$f(m) = \begin{cases} -\epsilon m^2 + c m^{\lambda-1} & \text{for } m k_c > 1 \\ -\epsilon m^2 + b m^4 & \text{for } m k_c < 1, \end{cases} \qquad (9)$$

where $k_c = aN^{1/\omega}$, $\epsilon = (T_c - T)/T_c$, $c =$ constant (independent of $\epsilon,\ N$), and $b = \langle k^4\rangle/\langle k^2\rangle^2$. For $3 < \lambda < 5$, an interesting cutoff-dependent FSS behavior at T_c is expected, which disappears far from T_c but in finite systems it can still survive to lead an anomalous FSS behavior near T_c.

Using $\xi_x \sim 1/|\Delta f(m_x)| \sim N$ and $\epsilon_x \sim N^{-\bar{\nu}_x}$ (where $x = c,\ q,\ *$), we get three scaling regimes as follows:

$$m = \begin{cases} \sim \epsilon^{\beta} & \text{for } \epsilon > \epsilon_* \\ \sim \left(\frac{\epsilon}{b}\right)^{\frac{1}{2}} & \text{for } \epsilon_c < \epsilon \le \epsilon_* \\ \sim (bN)^{-\frac{1}{4}} & \text{for } \epsilon \le \epsilon_c, \end{cases} \qquad (10)$$

where $\beta = 1/(\lambda-3)$, $\epsilon_* \sim b^{1/(1-2\beta)} \sim N^{-1/\bar{\nu}_*}$, and $\epsilon_c \sim (b/N)^{1/2} \sim N^{-1/\bar{\nu}_c}$.

Based on the definition of b and the cutoff scaling behavior, $k_c \sim N^{1/\omega}$, $b \sim N^{(5-\lambda)/\omega}$, so that $1/\bar{\nu}_* = (\lambda-3)/\omega$ and $1/\bar{\nu}_c = \left(1 - \frac{5-\lambda}{\omega}\right)/2$. For the comparison of the quenched case [8], where $1/\bar{\nu}_q = (\lambda-3)/(\lambda-1)$ is independent of ω, the critical exponents of Ising model in SFNs are summarized in Table 1.

As shown in Fig. 3, we can collapse numerical data in two ways, based on the scenario of three scaling regimes. For slightly better scaling collapse, we use the value of $b \equiv \langle k^4\rangle$ directly from empirically generated finite networks as well as the network size N, instead of simply assuming the scaling relation $b \sim N^{\frac{(5-\lambda)}{\omega}}$ for $N \gg 1$.

Fig. 4 shows that b and T_c have some finite-size corrections to their scaling, which get smaller as N increases. Thus, data collapse using only N shows asymptotically the same result as that using both b and N.

Due to long simulation time, we test up to $N = 64000$, and numerical data contain some extra finite-size corrections to the asymptotic scaling of m from small size systems. Although three scaling regimes are not directly and clearly observed from raw data plots of m (see Fig. 5), there is a clear evidence of the separation of three scaling regimes, I, II, and III, as predicted in the previous section, using the FSS technique carefully and support our previous analytic results with relatively small system sizes.

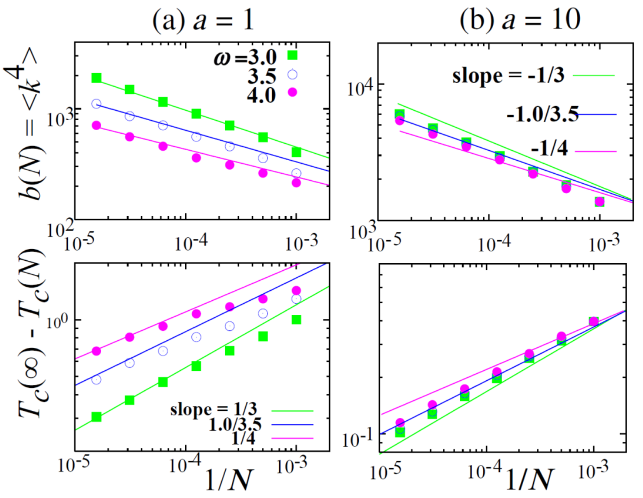

Fig. 4. (Color online) For $\lambda = 4.0$ with $\omega = 3.0$, 3.5, and 4.0, two different values of the coefficient a are considered to investigate how $b(N)$ (top) and $T_c(\infty) - T_c(N)$ (bottom) scale with N, respectively, in deterministic annealed SFNs as (a) $a = 1$ and (b) $a = 10$.

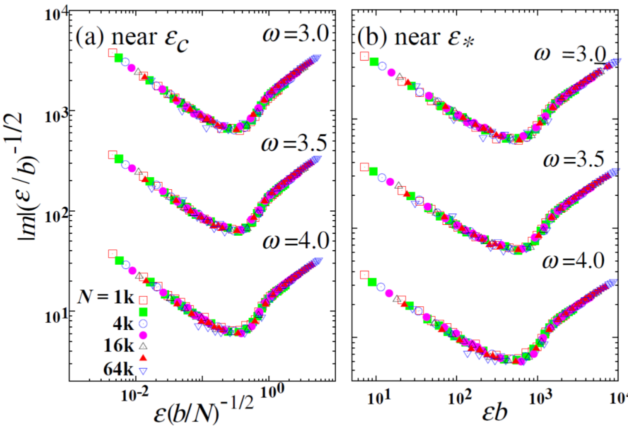

Fig. 5. Scaling collapse of m/m_x *vs.* ϵ/ϵ_x in deterministic annealed SFNs [10] for $\lambda = 4.0$. (a) near ϵ_c and (b) near ϵ_* using b, N and $k_c = aN^{1/\omega}$, where $a = 10$. Each dataset is shifted vertically in order to avoid an overlap and data are averaged over 10^5 Monte Carlo (MC) time steps for $N < 10^4$ and 10^4 MC time steps for $N > 10^4$, respectively, after the equilibration.

Based on the FSS conjecture for the Ising model on annealed SFNs (see Fig. 3) and the scaling relations summarized in Table 1, $m_c \sim (\epsilon_c/b)^{1/2} \sim (bN)^{-1/4}$ and $m_* \sim \epsilon_*^{\beta} \sim b^{\beta/(1-2\beta)}$, with $\beta = 1.0$ for $\lambda = 4.0$. In the other words, near ϵ_c, $(m/m_c)/(\epsilon/\epsilon_c)^{1/2} \sim m(\epsilon/b)^{-1/2}$ *vs.* $(\epsilon/\epsilon_c) \sim \epsilon(b/N)^{1/2}$, and near ϵ_*, $(m/m_*)/(\epsilon/\epsilon_*)^{1/2} \sim m(\epsilon/b)^{-1/2}$ *vs.* $(\epsilon/\epsilon_*) \sim \epsilon b$, respectively (see Fig. 5). For convenience sake, we note that the definition of the order parameter in numerical simulations is slightly different from that in analytic calculations, $m_{\text{MC}} = \sum_i s_i/N$, whereas $m_{\text{th}} = \sum_i k_i s_i/z_1 N$. It is numerically confirmed that they exhibit the same scaling behaviors (see Fig. 6).

Fig. 7 shows the relative standard deviation (RSD) of m, $\Delta m/\langle|m|\rangle_t$, and the Binder's cumulant, $U_4 = 1 - \frac{\langle m^4\rangle_t}{3\langle m^2\rangle_t^2}$, cross the same value as theoretical value of T_c in the horizontal axis, T, respectively. Here $\langle x\rangle_t$ means the temporal average in its equilibrium state.

The signature of the regime II (broadening of the flat region) is seen in Fig. 5 for $\omega > \omega_{\text{nat}}$, compared to the case of natural cutoff ($\omega_{\text{nat}} = \lambda - 1$) where no flat region exists (only two scaling regimes with the same critical exponents as those of the Ising model on quenched SFNs [8]). For the $a = 1$ case, it is also observed that scaling collapse becomes worse as ω increases, which is attributed to huge finite-size effects on $k_c = N^{1/\omega}$ value and the FSS. Contrast to the $a = 1$ case, for the $a = 10$ case (Fig. 5), the flat region is clearly developed and get broader as N and ω increase, but there is some different type of finite-size effects on the cutoff scaling as taking $k_c = 10N^{1/\omega}$ ("a=10" is somehow too big), so that our data may exhibit the natural cutoff scaling behavior also for finite systems. Finite-size corrections for the $a = 1$ case are larger than those for the $a = 10$ case, which is even larger in stochastically generated annealed SFNs due to sample fluctuations. Therefore, it would be another interesting task to find an optimal value of a which generates the least effect on the FSS and enhance the cutoff scaling for finite-size systems.

IV. SUMMARY AND DISCUSSION

We have revisited the finite-size scaling (FSS) in scale-free networks (SFNs), in the context of the cutoff scaling of annealed SFNs, where we employed the Ising model. With the upper cutoff $k_c \sim N^{1/\omega}$ of the degree distribution $P(k) \sim k^{-\lambda}$ for an annealed SFN of finite size N, we proposed the ω-dependent heterogeneous (also λ-dependent) FSS theory of Ising model for $3 < \lambda < 5$ due to the divergence of the coefficient $b(\sim \langle k^4\rangle)$ of the m^4 term in Landau free energy of the order parameter m near $T_c = \langle k^2\rangle/\langle k\rangle$ as both $k_c \to \infty$ and $N \to \infty$.

It implies the same two-route scenario to the thermodynamic limit of Ising model as that of the contact process (CP) reported in [9,10,14], so that the discrepancy of

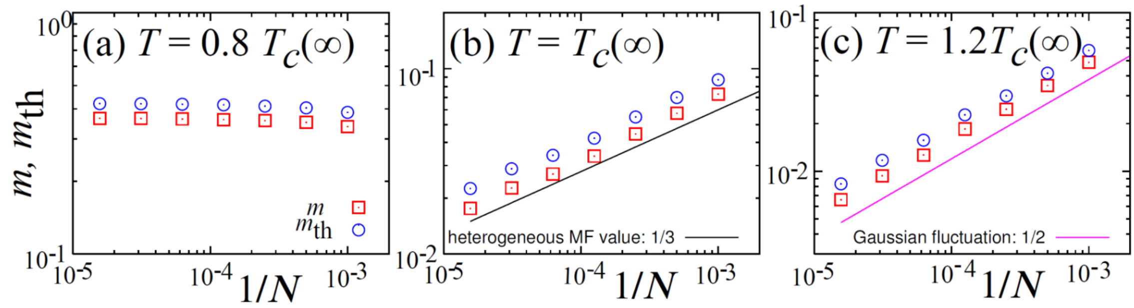

Fig. 6. (Color online) Double-logarithmic plots of $m(= m_{\rm MC})$ and $m_{\rm th}$ *vs.* $1/N$ for $\lambda = 4.0$ with $\omega = 3.0$ and $a = 5$ in $k_c = aN^{1/\omega}$: (a) $T = 0.8T_c$ (ordered; $|m| =$ const. > 0, independent of N), (b) $T = T_c$ (criticality, $|m| \sim N^{-[1+(5-\lambda)/\omega]/4}$), and (c) $T = 1.2T_c$ (disordered; $|m| \sim N^{-1/2}$), where the solid lines are drawn by the analytic calculations.

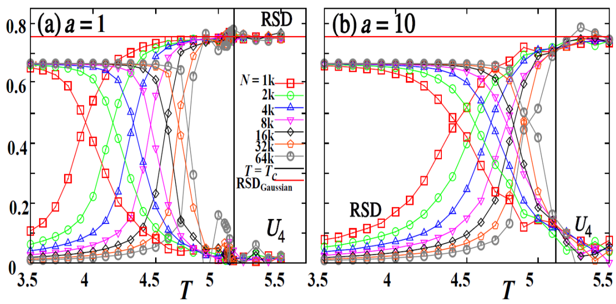

Fig. 7. (Color online) For $\lambda = 4.0$ with $\omega = \omega_{\rm nat}$, the RSD of m and the Binder's cumulant U_4 are plotted as a function of T, (a) $a = 1$ and (b) $a = 10$, where we can indicate the location of T_c within some reasonable error bars.

the FSS thoery in annealed and quenched SFNs is found for not only for the case of the CP but also the case of the Ising model. The strong cutoff issue in SF networks ($\omega \geq \omega_{\rm Herrero}$, where $\omega_{\rm Herrero} = \lambda$ [13]) are separately discussed in [11]. The role of the coefficient a in $k_c = aN^{1/\omega}$ is also under investigation [11], where the posed question is whether the "magic" (optimal) value of a for numerical tests exists or not.

Therefore, the FSS anlaysis is an essential task in network studies. Further FSS investigation will be necessary to obtain for better understanding of critical phenomena in real finite networks.

ACKNOWLEDGEMENTS

Some results presented here grew out of an enjoyable collaboration with Sang Hoon Lee in the early stage of our study for the Ising model on annealed SFNs [11].

REFERENCES

[1] M. E. J. Newman, SIAM Rev. **45**, 167 (2003).

[2] R. Albert and A.-L. Barabási, Rev. Mod. Phys. **74**, 47 (2002).

[3] S. N. Dorogovtsev and J. F. F. Mendes, Adv. Phys. **51**, 1079 (2002).

[4] S. Boccaletti, V. Latora, Y. Moreno, M. Chavez and D.-U. Hwang, Phys. Rep. **424**, 175 (2006).

[5] S. N. Dorogovtsev and J. F. F. Mendes, *Evolution of Networks: From Biological Nets to the Internet and WWW* (Oxford University Press, Oxford, 2003).

[6] S. N. Dorogovtsev, A. V. Goltsev and J. F. F. Mendes, Rev. Mod. Phys. **80**, 1275 (2008).

[7] M. E. J. Newman, S. H. Strogatz and D. J. Watts, Phys. Rev. E **64**, 026118 (2001).

[8] H. Hong, M. Ha and H. Park, Phys. Rev. Lett. **98**, 258701 (2007).

[9] M. Boguñá, C. Castellano and R. Pastor-Satorras, Phys. Rev. E **79**, 036110 (2009).

[10] J. D. Noh and H. Park, Phys. Rev. E **79**, 056115 (2009).

[11] S. H. Lee, M. Ha, H. Jeong, J. D. Noh and H. Park, Phys. Rev. E **80**, 051127 (2009).

[12] A. Aharony and A. B. Harris, Phys. Rev. Lett. **77**, 3700 (1996).

[13] C. P. Herrero, Phys. Rev. E **69**, 067109 (2004).

[14] C. Castellano and R. Pastor-Satorras, Phys. Rev. Lett. **100**, 148701 (2008).